

Magnetodielectric coupling in epitaxial Nd₂CoMnO₆ thin films with double perovskite structure

Avneesh Anshul, R. K. Kotnala, R. P. Aloysius, Anurag Gupta, and G. A. Basheed

Citation: *Journal of Applied Physics* **115**, 084106 (2014); doi: 10.1063/1.4866053

View online: <http://dx.doi.org/10.1063/1.4866053>

View Table of Contents: <http://scitation.aip.org/content/aip/journal/jap/115/8?ver=pdfcov>

Published by the AIP Publishing

Articles you may be interested in

[High Curie temperature BiInO₃-PbTiO₃ films](#)

J. Appl. Phys. **115**, 224105 (2014); 10.1063/1.4881797

[Structure and properties of epitaxial perovskite Pb\(Zr_{0.52}Ti_{0.48}\)O₃/La_{0.7}Sr_{0.3}MnO₃ heterostructures](#)

J. Appl. Phys. **111**, 07D718 (2012); 10.1063/1.3677866

[Magnetic and charge ordering properties of Bi_{0.6-x}\(RE\)_xCa_{0.4}MnO₃ \(0.0 < x < 0.6\) perovskite manganites](#)

J. Appl. Phys. **111**, 07E128 (2012); 10.1063/1.3675982

[Density of states, magnetic and transport properties of Nd doped two dimensional perovskite compound Sr₂CoO₄](#)

J. Appl. Phys. **111**, 07D708 (2012); 10.1063/1.3672825

[Magnetodielectric effect in double perovskite La₂CoMnO₆ thin films](#)

Appl. Phys. Lett. **91**, 042504 (2007); 10.1063/1.2762292


Instruments for Advanced Science

<p>Contact Hiden Analytical for further details:  www.HidenAnalytical.com  info@hiden.co.uk</p> <p>CLICK TO VIEW our product catalogue</p>	 <p>Gas Analysis</p> <ul style="list-style-type: none"> › dynamic measurement of reaction gas streams › catalysis and thermal analysis › molecular beam studies › dissolved species probes › fermentation, environmental and ecological studies 	 <p>Surface Science</p> <ul style="list-style-type: none"> › UHV TPD › SIMS › end point detection in ion beam etch › elemental imaging - surface mapping 	 <p>Plasma Diagnostics</p> <ul style="list-style-type: none"> › plasma source characterization › etch and deposition process reaction › kinetic studies › analysis of neutral and radical species 	 <p>Vacuum Analysis</p> <ul style="list-style-type: none"> › partial pressure measurement and control of process gases › reactive sputter process control › vacuum diagnostics › vacuum coating process monitoring
---	--	--	--	--

Magnetodielectric coupling in epitaxial $\text{Nd}_2\text{CoMnO}_6$ thin films with double perovskite structure

Avneesh Anshul,^{a)} R. K. Kotnala, R. P. Aloysius, Anurag Gupta, and G. A. Basheed^{a)}
 CSIR-National Physical Laboratory, Dr. K. S. Krishnan Road, New Delhi 110012, India

(Received 24 October 2013; accepted 1 February 2014; published online 25 February 2014)

Double perovskite $\text{Nd}_2\text{CoMnO}_6$ thin films have been grown epitaxially on SrTiO_3 substrates using pulsed laser deposition and their structural, magnetic, and dielectric properties were investigated. Temperature dependent dielectric (ϵ) constant is measured in the frequency range between 1 kHz and 1 MHz under applied magnetic fields up to 0.5 kOe. The dielectric constant exhibits an anomaly near to the Curie temperature which is independent of magnetic field and can be corroborated with a loop opening temperature in zero-field-cooled and field-cooled magnetization measurements. While, a linear relationship between magnetodielectric constant, $\delta\epsilon_{MD}$, and M^2 (magnetization) in the paramagnetic to ferromagnetic regime proves magnetodielectric coupling between ferroelectric and ferromagnetic orders in this single-phase perovskite system.
 © 2014 AIP Publishing LLC. [<http://dx.doi.org/10.1063/1.4866053>]

INTRODUCTION

Manganese based double perovskite oxide structures (RE_2BMnO_6 ; RE-rare earth element, and B-transition metal) offer a wide range of practical applications such as spintronic elements, magnetic storage,¹ and magnetoelectronics devices.² Control of magnetization (polarization) by an electric field (magnetic) in $\text{Nd}_2\text{CoMnO}_6$ (NCMO) double-perovskite ceramics possessing *ferroic* order in the same phase has prompted us to study their magnetodielectric (MD) coupling effects. In general, when the magnetic ordering breaks the inversion symmetry, the magnetodielectric coupling is expected to be large.³ The efficient magnetodielectric coupling between the ferroelectricity and magnetism is essential for the multi-control of the perovskite system which allows the magnetic control of polarization⁴ in order to design the logic architectures.⁵

The structural and magnetic properties of bulk $\text{Nd}_2\text{CoMnO}_6$ have been studied by Sazonov *et al.*^{6–8} and they showed that the NCMO consists of clusters of Co^{2+} and Mn^{4+} ions with different degrees of order and depend on the ionic order, NCMO exhibits first-order magnetic⁶ phase transition in an applied external magnetic field. The ferroelectric property of NCMO is originated by the off-center symmetry distortion caused by the ionic bond between Nd^{3+} and O^{2-} ions and the off-center displacement of lone-pair electrons of $6S^2 \text{Nd}^{3+}$ orbitals.⁹ The present study on NCMO thin film is to correlate the cation ordering¹⁰ and its magnetic order in comparison with bulk studies for its multifunctional applications.

EXPERIMENTAL DETAILS

In this article, first time, we report on the structural, magnetic, and magnetodielectric characterization of single-phase NCMO double perovskite thin films. NCMO thin films were grown on SrTiO_3 (STO (001)) substrate by pulsed laser deposition (PLD) using KrF ($\lambda = 248 \text{ nm}$) excimer laser.

These films were deposited at 700°C in an oxygen pressure of 0.6 Torr, with a laser fluence of $\sim 1.2 \text{ J cm}^{-2}$ with repetition rate of 4 Hz. The deposited thin films were cooled down (-10°C/min) to room temperature under an oxygen pressure of 100 Torr. The crystalline quality and epitaxial nature of the films were examined using a four-circle high resolution x-ray diffraction ($\text{CuK}\alpha$ radiation in $\theta-2\theta$, rocking curve) and Atomic Force Microscope (AFM) micrographs. The thickness of the films determined from XRD reflectivity measurements ranged between 20 and 100 nm.

Figure 1 shows the $\theta-2\theta$ XRD pattern of NCMO thin film (100 nm thick) grown on STO(001) substrate. Only (00 l) reflections of the perovskite structure are observed apart from the substrate peaks in the XRD. The lattice parameter value ($c = 3.897 \pm 0.001 \text{ \AA}$) is obtained and the lattice mismatch (of +0.2%) with compressive strain from the data based on the pseudocubic perovskite structure. A rocking-curve recorded from the (002) reflection of NCMO thin film (Fig. 1(a)) with a full-width at half maximum (FWHM) of 0.008° which indicates the high degree of crystalline orientation of these films.¹¹ Whereas, the bulk⁸ NCMO double perovskite with monoclinic structure belongs to $P2_1/n$ (No. 14) space group^{7,8} and has unit cell parameters $a = 5.4104 \text{ \AA}$, $b = 5.5405 \text{ \AA}$, and $c = 7.6613 \text{ \AA}$.

Dielectric properties of the NCMO films as a function of temperature and magnetic field were measured in Wayne Kerr 6500B system by depositing indium dots onto NCMO/ Nb:SrTiO_3 structure in the frequency range from 1 kHz to 1 MHz. In this work, we have investigated the effect of *ferroic* orders on the dielectric properties by measuring the sample capacitance as a function of temperature and magnetic field and quantifying the effect of MD coupling.

RESULTS AND DISCUSSION

Dielectric measurements of NCMO show a peak at 585 K indicating ferroelectric-paraelectric phase transition (T_{FE}) (shown in Fig. 2(a)). The decrease of the dielectric

^{a)}Electronic addresses: basheedga@nplindia.org and avneesh.anshul@gmail.com

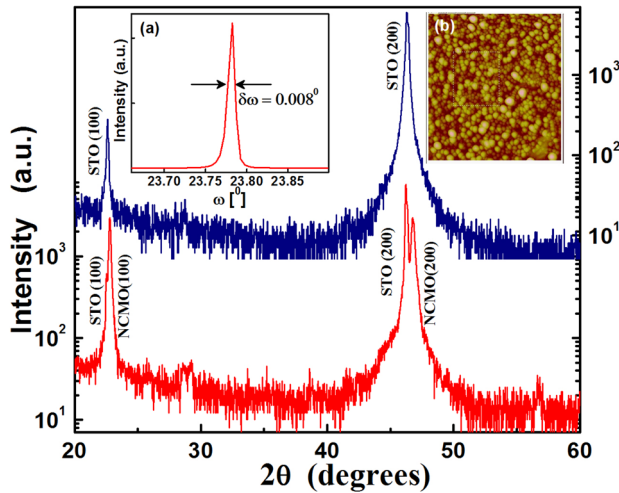


FIG. 1. X-ray diffraction pattern of $\text{Nd}_2\text{CoMnO}_6$ thin film sample grown on SrTiO_3 (001) substrate. Inset figures (a) and (b) show the rocking-curve of the (002) reflection for NCMO thin film and AFM micrograph.

constant (ϵ) with increasing frequency is caused by the inability of various polarization contributions to follow the change of the applied electric field, leading to lower dielectric constants and loss (Fig. 2(b)) at higher frequencies.¹² At higher temperature i.e., above T_{FE} , distortion stabilizes to symmetric and unpolarized state. Whereas, below T_{FE} , electron density of Nd^{3+} becomes more pronounced to hybridize $\text{Co}^{2+}/\text{Mn}^{4+}$, leads to exclusion of s-electron from bonding, imparts significant anisotropic structural distortion in NCMO thin films. The ferroelectric loop of NCMO thin film could not be measured due to leakage current characteristics and it

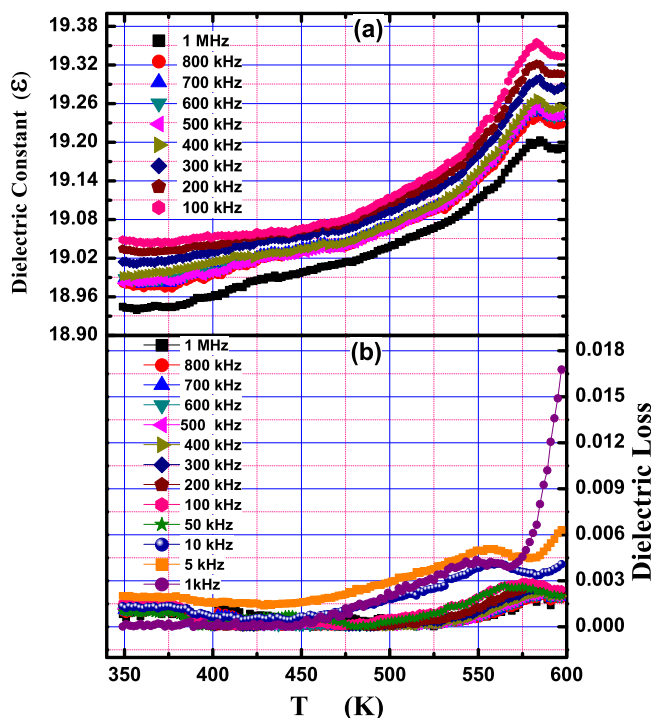


FIG. 2. Temperature dependence of dielectric constant of $\text{Nd}_2\text{CoMnO}_6$ thin film measured at different frequencies. (b) Dielectric loss as a function of temperature.

could be due to the existence of Mn^{2+} and oxygen vacancies.¹³

The magnetodielectric constant is defined as $\delta\epsilon_{MD} \equiv [\epsilon(H) - \epsilon(0)]/\epsilon(0)$, where $\epsilon(H)$ and $\epsilon(0)$ are the dielectric constants (ϵ) under applied field and zero applied magnetic fields. The temperature dependence of $\delta\epsilon_{MD}$ for 0.1 kOe and 0.5 kOe magnetic fields is shown in Fig. 3. At zero field, the dielectric constant increases steeply as shown in Figs. 3(a)–3(c) until the temperature reaches to 158 K which is near to the ferromagnetic transition temperature (T_{FM}). Whereas, above the *critical* temperature regime, it start decreases and comes to a constant value. Moreover, ferromagnetic transition temperature (T_{FM}) is independent of the applied magnetic field as shown in the left panel of Fig. 3.

In order to understand the origin of magnetic field induced dielectric constant in NCMO thin films and anomalies in the dielectric constant due to the magnetic ordering, Ginzburg-Landau theory of phase transitions is used.¹⁴ Smolenskii *et al.*^{15,16} showed the effect of dielectric constant (ϵ) on the magnetic order of ferroelectromagnets in the temperature range where $T_{FM} \ll T_{FE}$ and its free energy (F) may be written as

$$F(P, M) = F_0 + \alpha P^2 + \beta P^4 - PE + \alpha' M^2 + \beta' - MH + \gamma P^2 M^2, \quad (1)$$

where P and M are the electric polarization and magnetization and α , α' , β , β' , and γ are the coupling coefficients.¹⁷ H and E are external magnetic and electric fields, respectively. From the above expression, the difference of the relative dielectric constant below T_{FM} is proportional to the square of the magnetic-order parameter as

$$\delta\epsilon_{MD} \sim \gamma M^2 \quad (2)$$

$\delta\epsilon_{MD}$ depends on the sign of the magnetoelectric interaction constant γ , which is fairly high in the vicinity of critical temperature region.

Figure 4 shows the magnetic-field effect on the dielectric constant of the NCMO thin film as the application of magnetic fields induces the suppression of ϵ near T_{FM} with increasing fields. The magnetic field induced change in ϵ becomes a maximum at T_{FM} . In the NCMO system, Co^{2+} and Mn^{4+} ions are localized in distinct planes leading to a polar oxide perovskite system with strong local polarization. Near to the ferromagnetic transition temperature T_{FM} , the magnetic fluctuations lead to an optimization of coupling between electric (E) and magnetic (M) order parameters.¹² Since the ferroelectric transition temperature T_{FE} is far away from the ferromagnetic T_{FM} , the $\gamma P^2 M^2$ term in Eq. (1) is significant in the vicinity of T_{FM} .¹⁸ The magnetodielectric effect is small due to the uniform magnetization which cannot couple to the short wavelength polarization order parameter except for few magnetic excitations.

To clarify the magnetic order present in NCMO with respect to Co^{2+} and Mn^{4+} ionic ordering, we performed magnetization measurements by the use of Quantum Design Superconducting Quantum Interference Device (SQUID). Figure 5(a) shows the temperature dependent magnetization

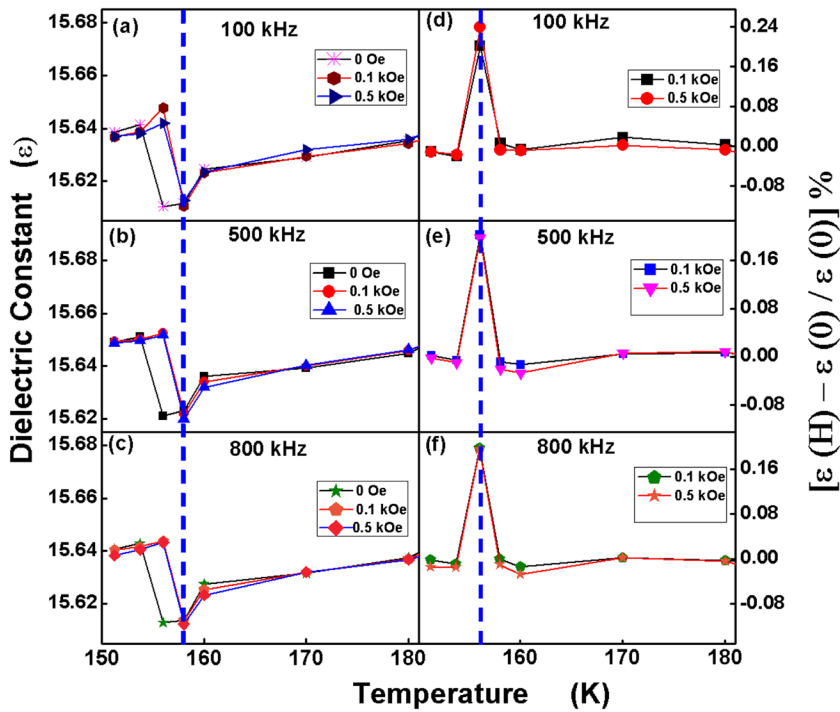


FIG. 3. Temperature dependence of dielectric constant [(a)–(c)] and $\delta\epsilon_{MD} \equiv [\epsilon(H) - \epsilon(0)]$ of $\text{Nd}_2\text{CoMnO}_6$ [(d)–(f)] thin film at various frequencies under the applied magnetic fields of 0.1 kOe and 0.5 kOe.

of NCMO thin film in the temperature (T) range $4.2 \leq T \leq 300$ K as induced after zero-field-cooled (ZFC) to $T = 4.2$ K by external magnetic field of $\mathbf{H}_{ext} = 10$ kOe. Large bifurcation between ZFC ($m^{ZFC}(T)$) and field-cooled FC ($m^{FC}(T)$) curves and a cusp as shown in Fig. 5 indicates a large magnetic anisotropy and competition between $m^{FC}(T)$ and Coercive field, $H_C(T)$, respectively. The NCMO thin film shows a typical ferromagnetic behavior below 174.5 K which arises from ordered arrangement of the CoO_6 and MnO_6 octahedra due to the positive exchange interactions between Co^{2+} (HS $\Rightarrow d^3$, $S = 3/2$) and Mn^{4+} (HS $\Rightarrow d^3$, $S = 3/2$), where HS is the high spin state of each ion. The paramagnetic to ferromagnetic phase transition (Fig. 5(d)) observed at $T_{FM} = 174.5$ K, which is close to the bulk^{6,8} value. Fig. 5(c) shows that magnetic susceptibility obeys the

Curie-Weiss law Weiss constant, $\Theta = +151$ K, also indicates that the interaction between Co^{2+} and Mn^{4+} is ferromagnetic type. The measured saturation magnetization at 5 K is $1.04 \mu_B$ /unit cell, which is smaller compared to bulk due to the epitaxial strain¹⁹ developed during deposition and anti-site disorder of the Co^{2+} and Mn^{4+} ions.^{18,20} The bifurcation between ZFC and FC is apparent at an irreversible temperature (T_{irr}), which is the temperature value at which the irreversible magnetic moment, defined as $\Delta m = m^{FC} - m^{ZFC}$, becomes different from zero, indicating the onset of a freezing process. The irreversible (T_{irr}) temperature decreases as \mathbf{H}_{ext} (=10 Oe, 100 Oe, and 1 k Oe) increases based on

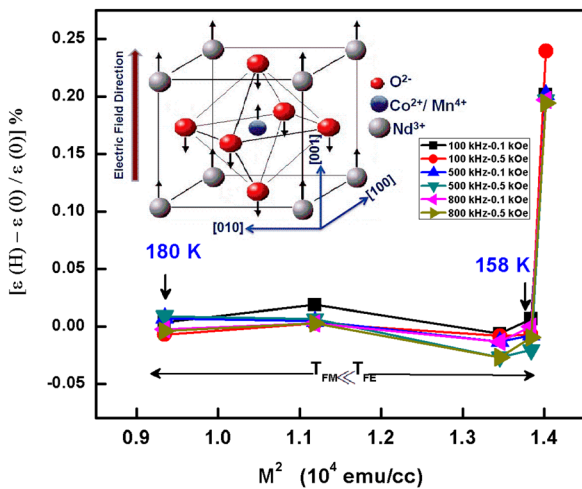


FIG. 4. Temperature dependence of dielectric constant of $\text{Nd}_2\text{CoMnO}_6$ thin film at various frequencies for 0.1 kOe and 0.5 kOe applied external magnetic field. Inset shows the magnetic structure of $\text{Nd}_2\text{CoMnO}_6$ perovskite thin film.

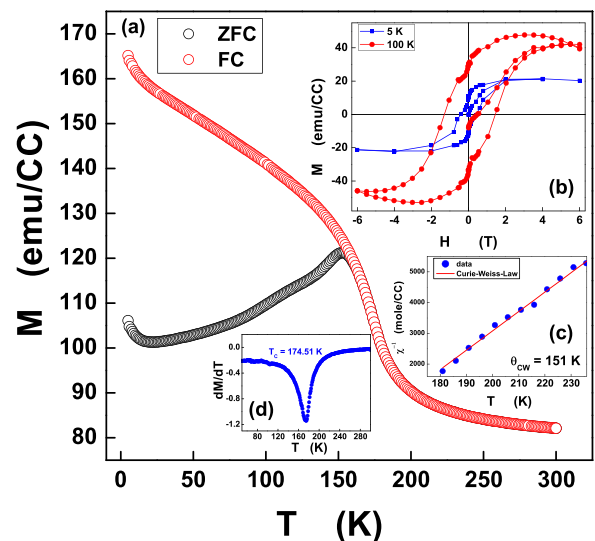


FIG. 5. (a) Field-cooled and zero-field-cooled magnetization as a function of temperature taken in an external applied field of 10 kOe. (b) Hysteresis cycles at 5 K and 100 K for parallel applied magnetic field. (c) Inverse DC susceptibility as function of temperature along with Curie-Weiss law fit. (d) Temperature dependence of magnetization for T_{FM} determination.

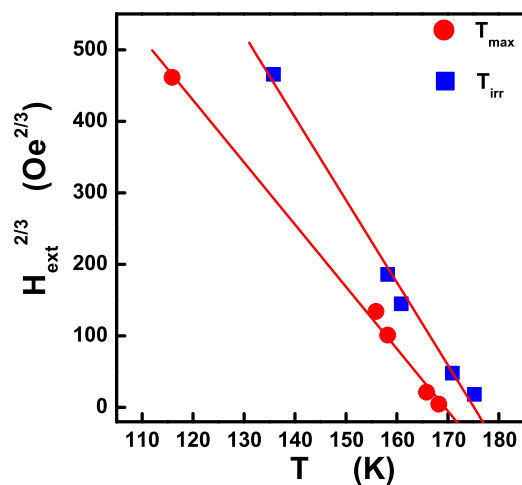


FIG. 6. Experimentally observed values of magnetic irreversible temperature (T_{irr}) fitted with the AT line ($T_{irr} \propto H_{ext}^{2/3}$) equation.

$T_{irr} \propto H_{ext}^{2/3}$ equation.²¹ Fig. 6 shows the field dependence based on *Almeida-Thouless* (AT)^{21,22} line in which T_{irr} and T_{max} (determined by m^{ZFC}) plotted against H_{ext} and follows the AT line. The linear extrapolation of AT lines of T_{max} (and T_{irr}) will determine the spin-freezing temperature, T_f , and it is equal to 172 ± 1 K which proves that the *spin-glass* state co-exists along with ferromagnetic order in double-perovskite NCMO thin films.

CONCLUSION

In summary, we have studied the effect of magnetic field on the dielectric properties of $\text{Nd}_2\text{CoMnO}_6$ thin films to understand the nature of magnetodielectric coupling. The NCMO thin films showed ferromagnetic ordering with a transition temperature of 175 K and ferroelectric transition temperature of 585 K. The transition from ferroelectric to paraelectric nature is found to be independent of the frequency at least in the range from 1 kHz to 1 MHz. The large bifurcation between ZFC and FC curves with a cusp at 172 K; and a decrease of irreversible temperature (T_{irr}) with applied magnetic field proves the *spin-glass* like behavior with long-range ferromagnetic order (Co^{2+} - O^{2-} - Mn^{4+}) co-exists in NCMO thin films. An anomaly in $\epsilon(T)$ at the magnetic ordering temperatures indicates the presence of magnetodielectric coupling effect in NCMO double perovskite thin films.

ACKNOWLEDGMENTS

A. Anshul thanks to CSIR, India, for providing CSIR Nehru fellowship to carry out his research work. G.A.B. is thankful to Director NPL for his support. A.A. and G.A.B. are thankful to Dr. S. Srinath, University of Hyderabad, Hyderabad, Dr. Sanjeev Kumar, TIFR, Bombay, and Dr. R. J. Chaudhary, UGC-DAE CSR, Indore, for their help in sample characterization.

- ¹Y. Ohno, D. K. Young, B. Beschoten, F. Matsukura, H. Ohno, and D. D. Awschalom, *Nature (London)* **402**, 790 (1999).
- ²K. F. Wang, J.-M. Liu, and Z. F. Ren, *Adv. Phys.* **58**, 321 (2009).
- ³Y. Yang, J.-M. Liu, H. B. Huang, W. Q. Zou, P. Bao, and Z. G. Liu, *Phys. Rev. B* **70**, 132101 (2004).
- ⁴T. Kimura, T. Goto, H. Shintani, K. Ishizaka, T. Arima, and Y. Tokura, *Nature (London)* **426**, 55 (2003).
- ⁵M. Gajek, M. Bibes, S. Fusil, K. Bouzehouane, J. Fontcuberta, A. Barthélémy, and A. Fert, *Nature Mater.* **6**, 296 (2007).
- ⁶A. P. Sazonov, I. O. Troyanchuk, M. Kopcewicz, V. V. Sikolenko, U. Zimmermann, and K. Baerner, *J. Phys.: Condens. Matter* **19**, 046218 (2007).
- ⁷A. P. Sazonov, I. O. Troyanchuk, D. P. Kozlenko, A. M. Balagurov, and V. V. Sikolenko, *J. Magn. Magn. Mater.* **302**, 443 (2006).
- ⁸A. P. Sazonov, I. O. Troyanchuk, V. V. Sikolenko, H. Szymczak, and K. Baerner, *Phys. Status Solidi B* **244**, 3367 (2007).
- ⁹A. Ciucivara, B. Sahu, and L. Kleinman, *Phys. Rev. B* **76**, 064412 (2007).
- ¹⁰M. P. Singh, K. D. Truong, and P. Fournier, *Appl. Phys. Lett.* **91**, 042504 (2007).
- ¹¹J. H. Haeni, P. Irvin, W. Chang, R. Uecker, P. Reiche, Y. L. Li, S. Choudhury, W. Tian, M. E. Hawley, B. Craigo, A. K. Tagantsev, X. Q. Pan, S. K. Streiffer, L. Q. Chen, S. W. Kirchoefer, J. Levy, and D. G. Schlom, *Nature (London)* **430**, 758 (2004).
- ¹²G. Lawes, A. P. Ramirez, C. M. Varma, and M. A. Subramanian, *Phys. Rev. Lett.* **91**, 257208 (2003).
- ¹³C. Wang, M. Takahashi, H. Fujino, X. Zhao, E. Kume, T. Horiuchi, and S. Sakai, *J. Appl. Phys.* **99**, 054104 (2006).
- ¹⁴*Physics of Ferroelectrics: A Modern Prospective*, edited by K. M. Rabe, C. H. Ahn, and M. Triscone (Springer-Verlag Series, 2007), and references therein.
- ¹⁵G. A. Smolenskii and I. E. Chupis, *Sov. Phys.* **25**, 475 (1982).
- ¹⁶G. A. Smolenskii, *Fiz. Tverd. Tela (Leningrad)* **4**, 1095 (1962) [*Sov. Phys. Solid State* **4**, 807 (1962)]; A. I. Mitsek and G. A. Smolenskii, *ibid.* **4**, 2620 (1963).
- ¹⁷T. Kimura, S. Kawamoto, I. Yamada, M. Azuma, M. Takano, and Y. Tokura, *Phys. Rev. B* **67**, 180401 (2003).
- ¹⁸C. A. F. Vaz, J. Hoffman, C. H. Ahn, and R. Ramesh, *Adv. Mater.* **22**, 2900 (2010).
- ¹⁹V. V. Lazenka, A. F. Ravinski, I. I. Makoed, J. Vanacken, G. Zhang, and V. V. Moshchalkov, *J. Appl. Phys.* **111**, 123916 (2012).
- ²⁰A. L. Cornelius, B. E. Light, and J. J. Neumeier, *Phys. Rev. B* **68**, 014403 (2003).
- ²¹J. R. L. De Almeida and D. J. Thouless, *J. Phys. A* **11**, 983 (1978).
- ²²M. Gabay and G. Toulouse, *Phys. Rev. Lett.* **47**, 201 (1981).